Proceedings of the 4th Asian Workshop on First-Principles Electronic Structure Calculations
Taipei, Taiwan (2001)

Bandstructures of hole-doped cuprates; correlation with $T_{c\,\max}$

O.K. Andersen, E. Pavarini*, I. Dasgupta†, T. Saha-Dasgupta‡, and O. Jepsen.
Max-Planck-Institut für Festkörperforschung, D-70506 Stuttgart, Germany

Abstract. We have developed a down-folding proceedure based on the density-functional formalism and the muffin-tin-orbital method for deriving low-energy, single-particle orbitals. By application to many families of cuprate high-temperature superconductors, we have derived a simple, generic conduction-band Hamiltonian for these systems. The essential *materials-dependence* turns out to be contained in only *one* parameter, namely the *range,* $r \sim t'/t$, of the hopping integrals in the CuO_2-layer. This range-parameter is controlled by the energy of a socalled *axial* (or perpendicular) orbital, a hybrid between Cu $4s$, Cu $3d_{3z^2-1}$, apical-oxygen $2p_z$, and farther orbitals such as La $5d_{3z^2-1}$. The axial orbital is also the vehicle for hopping perpendicular to the layer and it provides a characteristic $\cos k_x - \cos k_y$ dependence which has important consequences for perpendicular transport and tunneling. We observe that the materials with the larger hopping range, and hence with the axial orbital more localized onto the CuO_2-layers, have the higher $T_{c\,\max}$. This includes materials with multiple CuO_2-layers. Possible reasons for this correlation will be mentioned. This paper is an extended version of Ref. [1].

1 Introduction

The mechanism of high-temperature superconductivity (HTSC) in the hole-doped cuprates remains a puzzle [2]. Many families with CuO_2-layers have been synthesized and all exhibit a phase diagram with T_c going through a maximum as a function of doping. The prevailing explanation is that at low doping, superconductivity is destroyed with rising temperature by the loss of phase coherence, and at high doping by pair-breaking [3]. For the *materials-*dependence of T_c at optimal doping, $T_{c\,\max}$, the only known, but not understood, systematics is that for materials with multiple CuO_2-layers, such as $HgBa_2Ca_{n-1}Cu_nO_{2n+2}$, $T_{c\,\max}$ increases with the number of layers, n, until $n \sim 3$. There is little clue as to why for n fixed, $T_{c\,\max}$ depends strongly on the family, *e.g.* why for n=1, $T_{c\,\max}$ is 40 K for La_2CuO_4 and about 90 K for $Tl_2Ba_2CuO_6$ and $HgBa_2CuO_4$, although the Neel temperatures are fairly similar. A wealth of structural data has been obtained, and correlations between structure and T_c have often been looked for as functions of doping, pressure, uniaxial strain, and family. However, the large number of structural and compositional parameters makes it difficult to find what besides doping controls the superconductivity. Recent studies of thin epitaxial $La_{1.9}Sr_{0.1}CuO_4$ films concluded that the distance between the charge reservoir and the CuO_2-plane is the key structural parameter determining the normal state and superconducting properties [4].

Most theories of HTSC are based on a Hubbard model with *one* Cu $d_{x^2-y^2}$-like orbital per CuO_2-unit. The one-electron part of this model is, in the **k**-representation:

$$\varepsilon(\mathbf{k}) = -2t(\cos k_x + \cos k_y) + 4t' \cos k_x \cos k_y - 2t''(\cos 2k_x + \cos 2k_y) + \ldots, \qquad (1)$$

with t, t', t'', ... denoting the hopping integrals (≥ 0) on the square Cu lattice (Fig. 1). For simplicity, we have set the lattice constant $a \equiv 1$. Early theories only took t into account, but the consistent results of local-density approximation (LDA) band-structure calculations [5] and angle-resolved photoemission spectroscopy (for overdoped, stripe-free materials) [6], have led to the current usage of including also t', with $t'/t \sim 0.1$ for La_2CuO_4 and $t'/t \sim 0.3$ for $YBa_2Cu_3O_7$ and $Bi_2Sr_2CaCu_2O_8$, whereby the constant-energy contours of expression (1) become rounded squares oriented in respectively the [11]- and [10]-directions. It is conceivable that the materials-dependence enters the Hamiltonian primarily via its one-electron part (1), and that this dependence is captured by LDA calculations. But it needs to be filtered out:

The LDA band structure of the best known, and only stoichiometric optimally doped HTSC, $YBa_2Cu_3O_7$, is more complicated than what can be described with the t-t' model. Nevertheless, previous careful analysis had shown [5] that the *low*-energy *layer*-related features, which are the only generic ones, can be described by a *nearest*-neighbor tight-binding model with the following *four* orthogonal orbitals per layer: Cu $3d_{x^2-y^2}$, Cu $4s$, O_a $2p_x$, and O_b $2p_y$. These orbitals, their energies, and hopping integrals are sketched in Fig. 1. In $\mathbf{k}$-space, the Hamiltonian is seen to be:

$$\begin{array}{cccc} |d,\mathbf{k}\rangle: & |s,\mathbf{k}\rangle: & |x,\mathbf{k}\rangle: & |y,\mathbf{k}\rangle: \\ \\ \varepsilon_d & 0 & 2t_{pd}\sin k_x/2 & -2t_{pd}\sin k_y/2 \\ 0 & \varepsilon_s & 2t_{sp}\sin k_x/2 & 2t_{sp}\sin k_y/2 \\ 2t_{pd}\sin k_x/2 & 2t_{sp}\sin k_x/2 & \varepsilon_p & 0 \\ -2t_{pd}\sin k_y/2 & 2t_{sp}\sin k_y/2 & 0 & \varepsilon_p \end{array} \tag{2}$$

and the constant-energy contours, $\varepsilon_i(\mathbf{k})=\varepsilon$, can therefore be expressed simply as [5]:

$$1-u-d(\varepsilon)+(1+u)\,p(\varepsilon)=\frac{v^2}{1-u+s(\varepsilon)} \tag{3}$$

in terms of the coordinates $u \equiv \frac{1}{2}(\cos k_x+\cos k_y)$ and $v \equiv \frac{1}{2}(\cos k_x-\cos k_y)$, and the quadratic functions

$$d(\varepsilon)\equiv\frac{(\varepsilon-\varepsilon_d)(\varepsilon-\varepsilon_p)}{(2t_{pd})^2} \qquad \text{and} \qquad s(\varepsilon)\equiv\frac{(\varepsilon_s-\varepsilon)(\varepsilon-\varepsilon_p)}{(2t_{sp})^2}, \tag{4}$$

which describe the coupling of $O_{a/b}\,p_{x/y}$ to respectively Cu $d_{x^2-y^2}$ and Cu s. The term proportional to $p(\varepsilon)$ in (3) describes the admixture of $O_{a/b}\,p_z$ orbitals for dimpled layers and

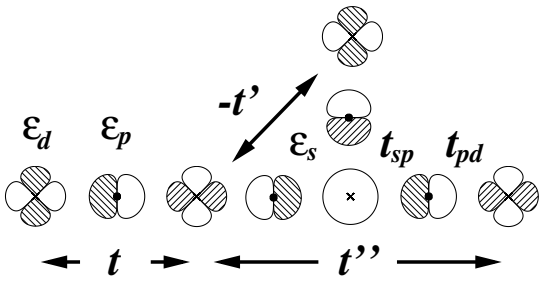

Figure 1: Relation between the long-ranged one-orbital model with parameters t, t', t'', etc. and the nearest-neighbor four-orbital model with parameters $\varepsilon_d-\varepsilon_p \sim 1\,\text{eV}$, $t_{pd} \sim 1.5\,\text{eV}$, $\varepsilon_s-\varepsilon_p \sim 4-16\,\text{eV}$, and $t_{sp} \sim 2\,\text{eV}$.

actually extends the four-orbital model to a six-orbital one [5]. For ε near the middle of the conduction band, $d(\varepsilon)$, $s(\varepsilon)$, and $p(\varepsilon)$ are positive, and the energy dependence of $d(\varepsilon)$ may be linearized ($\dot{d} > 0$), while those of $s(\varepsilon)$ and of $p(\varepsilon)$ may be neglected. Now, if ε_s were infinitely far above the conduction band, or t_{sp} vanishingly small, the right-hand side of (3) would vanish, with the result that the constant-energy contours would depend only on u. The dispersion of the conduction band near the Fermi level would thus be that of the one-orbital model (1) with $t = (1-p)/4\dot{d}$ and $t' = t'' = 0$. For realistic values of ε_s and t_{sp}, the conduction band attains Cu s-character proportional to v^2, thus vanishing along the nodal direction, k_x=k_y, and peaking at $(\pi, 0)$ where it is of order 10 per cent. The repulsion from the Cu s-band lowers the energy of the van Hove singularities and turns the constant-energy contours towards the [10]-directions. In a bilayer material, the bonding and antibonding subbands have ε_s-values split by $\mp t_{ss}^{\perp}$, and this same v^2-dependence therefore pertains to the inter-layer splitting.

In order to go from Eq. (3) to Eq. (1), $1/(1-u+s) \equiv 2r/(1-2ru)$ was expanded in powers of $2ru$, where

$$r \equiv \frac{1}{2(1+s)}. \tag{5}$$

This provided explicit expressions, such as:

$$t = \frac{1-p+o(r)}{4\dot{d}}, \quad t' = \frac{r+o(r)}{4\dot{d}}, \quad \text{and} \quad t'' = \frac{1}{2}t' + o(r), \tag{6}$$

for the hopping integrals of the one-orbital model in terms of the parameters of the four(six)-orbital model and the expansion energy $\sim \varepsilon_F$. Note that all intra-layer hoppings beyond nearest neighbors are expressed in terms of the *range*-parameter r. Although one may think of r as t'/t, this holds only for flat layers and when $r < 0.2$. When $r > 0.2$, the series (1) must be carried beyond t''. Dimpling is seen not to influence the range of the intra-layer hopping, but to reduce t through admixture of $O_{a/b}\, p_z$. In addition, it reduces t_{pd}.

2 Trends

Here, we shall generalize this analysis to all known families of HTSC materials using a new muffin-tin-orbital (MTO) method [7] which allows us to construct minimal basis sets for the low-energy part of an LDA band structure with sufficient accuracy that we can extract the materials dependence. This dependence, we find to be contained solely in ε_s, which is now the energy of the *axial* orbital, a hybrid between Cu s, Cu d_{3z^2-1}, apical-oxygen $O_c\, p_z$, and farther orbitals on *e.g.* La or Hg. The range, r, of the intra-layer hopping is thus controlled by the structure and chemical composition *perpendicular* to the CuO_2-layers. It turns out that the materials with the larger r (lower ε_s) tend to be those with the higher observed values of $T_{c\max}$. In the materials with the highest $T_{c\max}$, the axial orbital is almost pure Cu $4s$. It should be noted that r describes the *shape* of the non-interacting band in a 1 eV-range around the Fermi level, whose accurate position is unknown because we make no assumptions about the remaining terms of the Hamiltonian, inhomogeneities, stripes, a.s.o.

Fig. 2 shows the LDA bands for the single-layer materials La_2CuO_4, $Tl_2Ba_2CuO_6$, and $HgBa_2CuO_4$. Whereas the high-energy band structures are complicated and very different, the low-energy conduction bands shown by dashed lines contain the generic features. Most notably, the dispersion along $(0,0)-(\pi,0)$ is suppressed for the compounds with the higher

$T_{c\,\max}$, whereas the dispersion along $(0,0)-(\pi,\pi)$ is the same. This is the v^2-effect. The low-energy bands were calculated variationally with a single Bloch sum of Cu $d_{x^2-y^2}$-like zeroth-order muffin-tin orbitals (ZMTOs) constructed to be correct at an energy near half-filling. Hence, these bands agree with the full band structures merely to linear order and head towards the pure Cu $d_{x^2-y^2}$-levels at $(0,0)$, extrapolating across a multitude of irrelevant bands. As was explained in Refs. [7, 8], we could have made the fit abitrarily good by using a Cu $d_{x^2-y^2}$-like MTO of higher order, but this is undesirable because fitting the band structure over a wider energy range picks up non-generic features. Now, fourier-transformation of the low-energy conduction band (dashed) yields the hopping integrals shown on the right-hand side: In all cases $t \sim 0.45\,\mathrm{eV}$, $t'/t \sim 0.15$ for La_2CuO_4, but ~ 0.35 for the high-$T_{c\,\max}$ cuprates $Tl_2Ba_2CuO_6$ and $HgBa_2CuO_4$, and $t''/t' \sim 1/2$ in all cases, in agreement with Eq. (4).

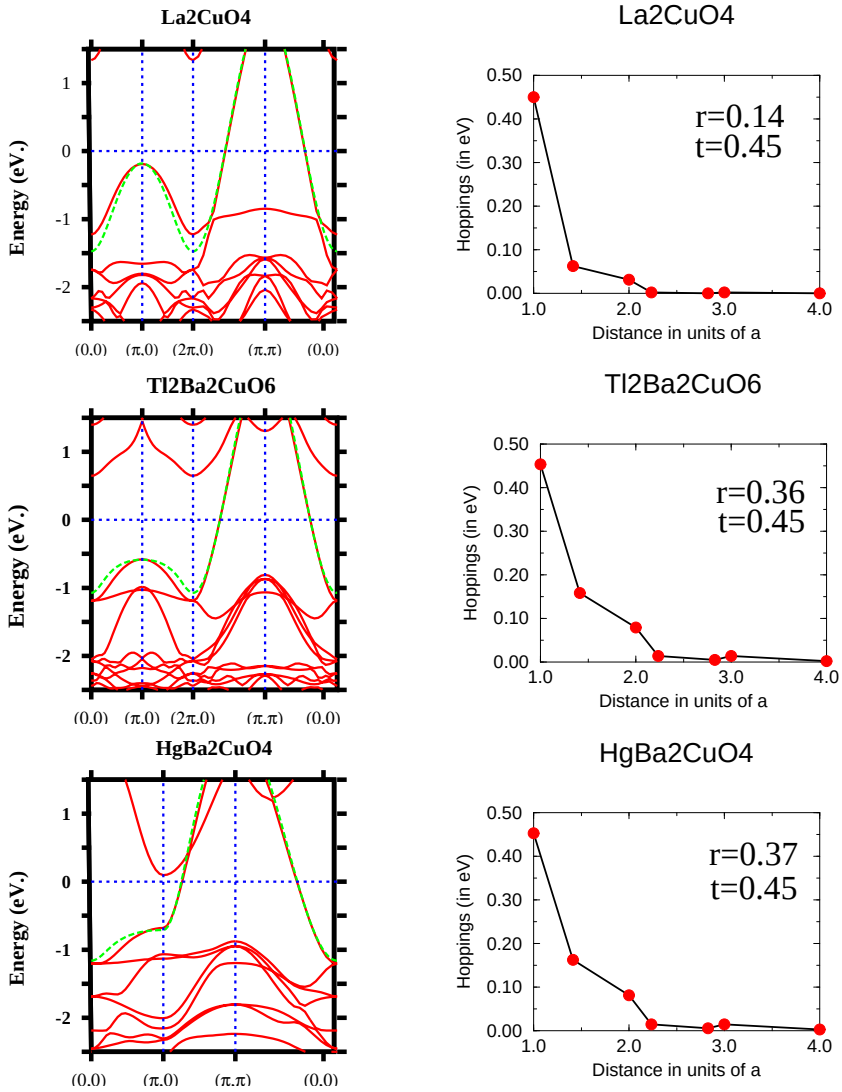

Figure 2: LDA bands (solid) and Cu $d_{x^2-y^2}$-like low-energy conduction band (dashed) for the bct-like cuprates La_2CuO_4 ($T_{c\,max} \sim 40\,\mathrm{K}$) and $Tl_2Ba_2CuO_6$ (85 K) for $k_z = \frac{\pi}{c}$, and for primitive tetragonal $HgBa_2CuO_4$ (90 K) for $k_z = \frac{\pi}{2c}$. *Right:* In-layer hopping integrals (t) for the low-energy band. $t \equiv t\,(a)$, $t' \equiv t\left(a\sqrt{2}\right)$, $t'' \equiv t\,(2a)$, a.s.o.

Fig. 3 shows the conduction-band orbitals of La_2CuO_4 and $HgBa_2CuO_4$ in the plane of the CuO_2-layer, the xy-plane. If one interprets the hopping integrals as overlap integrals for such an orbital, one may realize that the main signature of a larger t' is a larger amplitude at the oxygens which are second-nearest neighbors to the central copper. The strange-looking "hole" in the conduction-band orbital near the nearest-neighbor copper site for $HgBa_2CuO_4$ is, in fact, the outermost radial node of the diffuse Cu 4s-partial wave.

In Fig. 4 we show the conduction-band orbitals in the xz-plane, perpendicular to the CuO_2-layers. Starting from the central Cu atom and going in the x-direction, we see $3d_{x^2-y^2}$

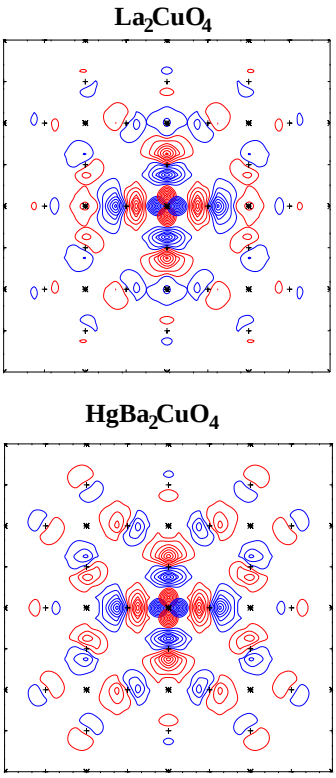

Figure 3: ZMTO conduction-band orbital in the CuO_2-layer for La_2CuO_4 and $HgBa_2CuO_4$.

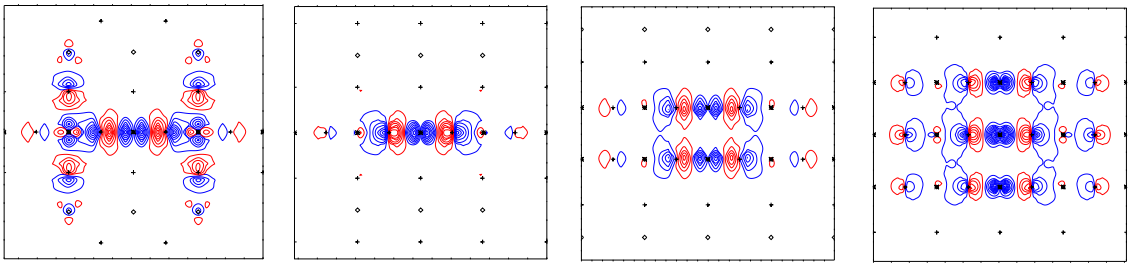

Figure 4: Conduction-band orbital in the xz-plane perpendicular to the layers for La_2CuO_4, $HgBa_2CuO_4$, and the bi- and triple-layer Hg-cuprates.

antibond to neighboring O_a $2p_x$, which itself bonds to $4s$ and, for La_2CuO_4, antibonds to $3d_{3z^2-1}$ on the next Cu. From here, and in the z-direction, we see $4s$ and, for La_2CuO_4, also $3d_{3z^2-1}$ antibond to $O_c\,2p_z$, which itself bonds to La orbitals, mostly $5d_{3z^2-1}$. For $HgBa_2CuO_4$ we find about the same amount of Cu $3d_{x^2-y^2}$ and $O_{a/b}\,2p_{x/y}$ character, but more Cu $4s$, negligible Cu $3d_{3z^2-1}$, much less $O_c\,2p_z$. In $HgBa_2CuO_4$, and also in $Tl_2Ba_2CuO_6$, the axial part of the conduction-band orbital is thus mainly the diffuse Cu $4s$.

The appearance of the conduction-band orbital makes it conceivable that all the in-layer hopping integrals and their materials-dependence can be described with a *generalized four-orbital model.* ZMTO calculations with downfolding to basis sets larger than one MTO per CuO_2 now confirm that in order to localize the orbitals to the extend that only nearest-neighbor hoppings are essential, one needs to add *one* orbital, Cu *axial,* to the three standard orbitals, Cu $3d_{x^2-y^2}$, $O_a\,2p_x$, and $O_b\,2p_y$. The corresponding four-orbital Hamiltonian is therefore the one described above in Fig. 1 and Eqs. (3-6). Note that we continue to call the energy of the axial orbital ε_s and its hopping to $O_a\,p_x$ and $O_b\,p_y$ t_{sp}.

Calculations with this four-orbital basis for many different materials show that of the four parameters, *only one,* the energy ε_s of the axial orbital, varies significantly [8]. This variation can be understood in terms of the following nearest-neighbor Hamiltonian in the representation of the Bloch sums of the following six orthonormal orbitals: Cu $3d_{x^2-y^2}$, Cu $3d_{3z^2-1}$, Cu $4s$, $O_a\,2p_x$, $O_b\,2p_y$, and the even linear combination of apical $O_c\,2p_z$ at $(0,0,zc)$ and $(0,0,-zc)$:

$\lvert d,\mathbf{k}\rangle$:	$\lvert z^2,\mathbf{k}\rangle$:	$\lvert \bar{s},\mathbf{k}\rangle$:	$\lvert x,\mathbf{k}\rangle$:	$\lvert y,\mathbf{k}\rangle$:	$\lvert \bar{c},\mathbf{k}\rangle$:
ε_d	0	0	$2t_{pd}\sin k_x/2$	$-2t_{pd}\sin k_y/2$	0
0	ε_{z^2}	0	$-2t_{pz^2}\sin k_x/2$	$-2t_{pz^2}\sin k_y/2$	$\sqrt{2}t_{cz^2}$
0	0	$\varepsilon_{\bar{s}}$	$2t_{sp}\sin k_x/2$	$2t_{sp}\sin k_y/2$	$\sqrt{2}t_{sc}$
$2t_{pd}\sin k_x/2$	$-2t_{pz^2}\sin k_x/2$	$2t_{sp}\sin k_x/2$	ε_p	0	0
$-2t_{pd}\sin k_y/2$	$-2t_{pz^2}\sin k_y/2$	$2t_{sp}\sin k_y/2$	0	ε_p	0
0	$\sqrt{2}t_{cz^2}$	$\sqrt{2}t_{sc}$	0	0	$\varepsilon_{\bar{c}}-t_{cc}c_xc_yc_z$

Here, $\varepsilon_{\bar{s}}$ and $\varepsilon_{\bar{c}}$ denote the energies of the pure Cu s- and $O_c\,p_z$-orbitals, and t_{sc} denotes the hopping between them. The energy of Cu d_{3z^2-1} is ε_{z^2} and its hopping integrals to $O_{a/b}\,p_{x/y}$ and $O_c\,p_z$ are respectively t_{pz^2} and t_{cz^2}. The La orbital will be included later, in Eq. (7). Although specific for bct La_2CuO_4, this Hamiltonian is easy to generalize.

Interlayer coupling mainly proceeds via t_{cc} between $O_c\,2p_z$ at $(0,0,zc)$ and its four nearest neighbors at $\left(\pm\frac{1}{2},\pm\frac{1}{2},\left(\frac{1}{2}-z\right)c\right)$. As a consequence, the k_z-dependence is contained in the term $t_{cc}c_xc_yc_z \equiv 8t_{cc}\cos\frac{k_x}{2}\cos\frac{k_y}{2}\cos\frac{ck_z}{2}$. In primitive tetragonal (t) materials, the CuO_2-layers are stacked on top of each other and this causes the corresponding term to be $\propto \cos ck_z$. E.g. in $HgBa_2CuO_4$, the interlayer coupling proceeds from $O_c\,2p_z$ at $(0,0,zc)$ via Hg $6s/6p_z$ at $(0,0,c/2)$ to $O_c\,2p_z$ at $(0,0,(1-z)\,c)$.

As long as $t_{pz^2}^2/t_{sp}^2 \ll \frac{\varepsilon_F-\varepsilon_{z^2}}{\varepsilon_{\bar{s}}-\varepsilon_F}$ and $t_{pd}^2/t_{sp}^2 \ll \frac{\varepsilon_F-(\varepsilon_p+\varepsilon_d)/2}{\varepsilon_F-(\varepsilon_p+\varepsilon_s)/2}$, downfolding of this Hamiltonian to a Cu $3d_{x^2-y^2}$-like one-orbital Hamiltonian yields Eqs. (3)-(6) with the energy of the axial orbital given by:

$$\varepsilon_s = \varepsilon_{\bar{s}} + \frac{2t_{sc}^2}{\varepsilon_F-\varepsilon_c}, \quad \text{where} \quad \varepsilon_c = \varepsilon_{\bar{c}} + \left(1+\frac{t_{sc}}{t_{sp}}\frac{t_{pz^2}}{t_{cz^2}}\right)^2 \frac{4\bar{r}t_{cz^2}^2}{\varepsilon_F-\varepsilon_{z^2}} - \frac{t_{c\,La}^2}{\varepsilon_{La}-\varepsilon_F} - t_{cc}c_xc_yc_z \quad (7)$$

is the energy of the $O_c\,p_z$-like 5-atom hybrid Cu d_{3z^2-1}-2$O_c\,p_z$-2 La. The expressions (7) for the energy of the axial orbital are illustrated by the diagram in Fig. 5.

In Fig. 6 we plot the r-values for single-layer materials against the distance $d_{\mathrm{Cu-O}_c}$ between Cu and apical oxygen. r, as given in terms of ε_s by Eqs. (4) and (5), increases with $d_{\mathrm{Cu-O}_c}$ because ε_s is lowered towards ε_F when the hoppings t_{cz^2} and t_{sc} from $\mathrm{O}_c\, p_z$ to $\mathrm{Cu}\, d_{3z^2-1}$ and to Cu s are weakened. Since $t_{cz^2} \propto d^{-4}_{\mathrm{Cu-O}_c}$ and $t_{sc} \propto d^{-2}_{\mathrm{Cu-O}_c}$, increasing the distance suppresses the $\mathrm{Cu}\, d_{3z^2-1}$ content, which is important in La_2CuO_4, but negligible in $Tl_2Ba_2CuO_6$ and $HgBa_2CuO_4$. This is also reflected in the slopes of the lines in Fig. 6 which, for each material, give r vs. $d_{\mathrm{Cu-O}_c}$. The strong slope for La_2CuO_4 explains the strained-film results [4], provided that r correlates with superconductivity. That the Bi-point does not fall on the La-line is an effect of Bi being different from La: $\mathrm{Bi}\, 6p_z$ couples stronger to $\mathrm{O}_c\, 2p_z$ than does $\mathrm{La}\, 5d_{3z^2-1}$. The figure shows that upon reaching $HgBa_2CuO_4$, r is saturated, $\varepsilon_s \sim \varepsilon_{\bar{s}}$, and the axial orbital is almost pure $\mathrm{Cu}\, 4s$.

Fig. 6 hints that for single-layer materials, r might correlate with the observed $T_{c\,\max}$.

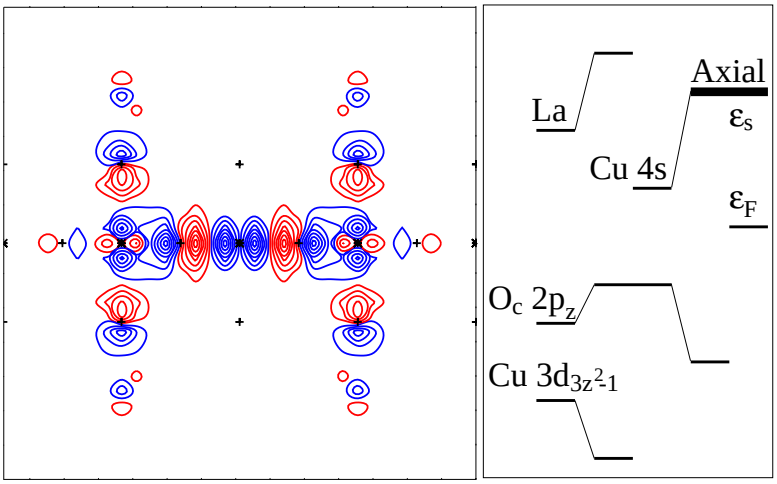

Figure 5: Conduction-band orbital for La_2CuO_4 in the xz-plane and a schematic diagram giving the energy ε_s of the axial orbital in terms of the energies of its constituents and their couplings.

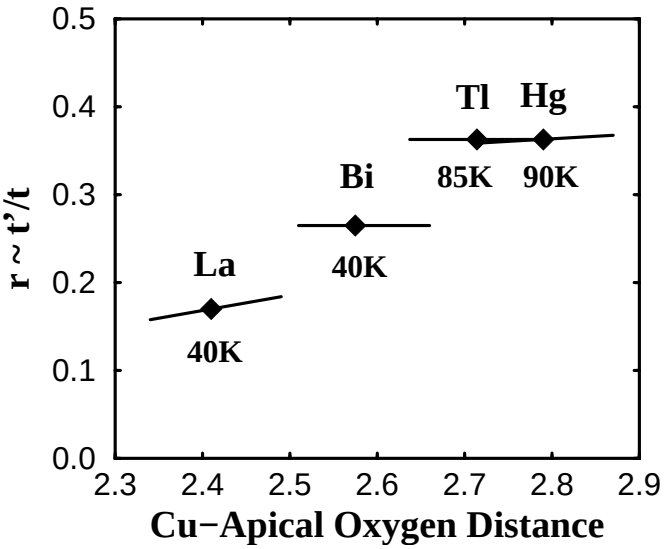

Figure 6: Calculated range parameter, r, for single-layer materials vs the distance between Cu and O_c (in Å). The lines result from rigid displacements of O_c.

But the experimental uncertainties of both $T_{c\max}$ and the structural parameters are such that we need better statistics. We therefore plot the observed $T_{c\max}$ against the calculated r-values for nearly all hole-doped HTSCs in Fig. 7. For the single-layer materials we observe a strong correlation between r and $T_{c\max}$, which seems to be continued in the *bonding* subband for the multilayer materials (filled squares). This indicates that the electrons are delocalized over the multilayer [11], and that $T_{c\max}$ increases with the number of layers for the *same* reason that it increases among single-layer materials; the multilayer is simply a means of lowering ε_s further, through the formation of Cu s-Cu s bonding states as seen in the bottom parts of Fig. 3. This is consistent with the celebrated pressure-enhancement [10] of T_c in $HgBa_2Ca_2Cu_3O_8$, and the fact [9] that $T_{c\max}$ drops from 92 K to 50 K when Y is replaced by the larger cation La in $YBa_2Cu_3O_7$. The r-values calculated for $LaBa_2Cu_3O_7$ are included in Fig. 7 and are seen to follow the trend! That $T_{c\max}$ eventually drops for an increasing number of layers, is presumably caused by loss of phase coherence. Coherent inter-layer coupling makes ε_s depend on k_z, and this passes onto the conduction band a k_z-dispersion $\propto v^2 \cos\frac{1}{2}k_x \cos\frac{1}{2}k_y \cos\frac{1}{2}ck_z$ in bct and $\propto v^2 \cos ck_z$ in tetragonal structures. Fig. 7 shows how the k_z-dispersion of r decreases when the axial orbital contracts to Cu $4s$.

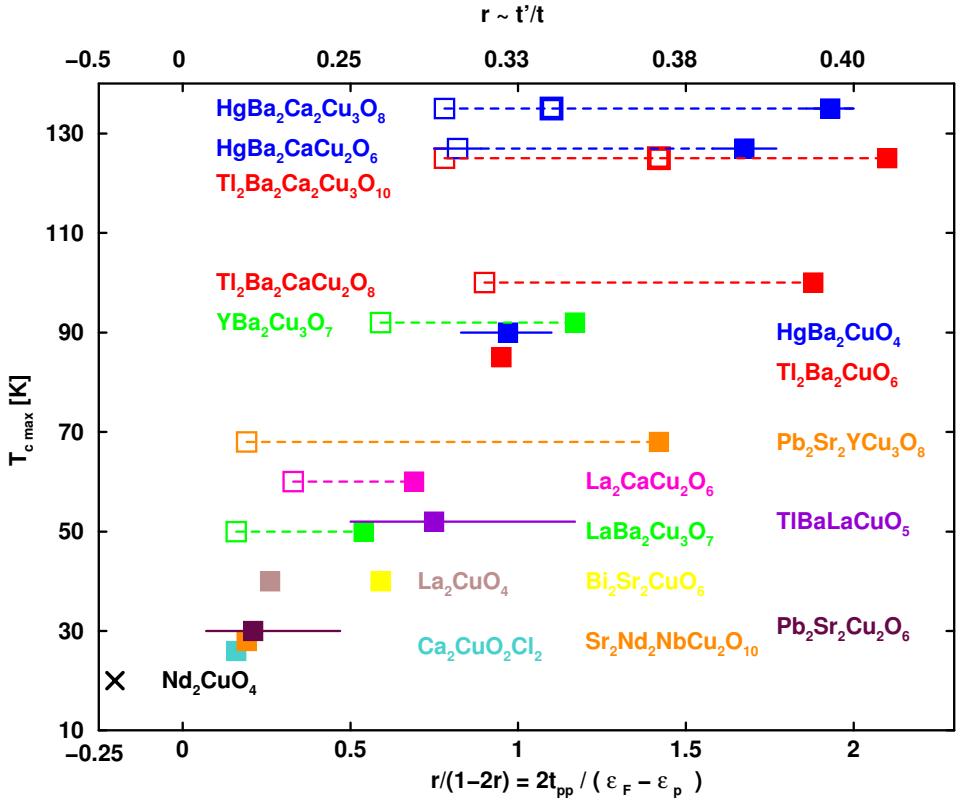

Figure 7: Correlation between calculated r and observed $T_{c\,\max}$. Filled squares: single-layer materials and most bonding subband for multilayers. Weak empty squares: most antibonding subband. Strong empty squares: nonbonding subband. Dotted lines connect subband values. Bars give k_z-dispersion of r in primitive tetragonal materials. The horizontal scale is linear in $\frac{r}{1-2r}$, which is proportional to the parameter t_{pp} in the three-orbital model obtained by downfolding of the axial orbital.

3 Conclusion

Our identification of an electronic parameter, r or ε_s, which correlates with the observed $T_{c\max}$ for all known types of hole-doped HTSC materials could be a useful guide for materials synthesis and a key to understanding HTSC. With current **k**-space renormalization-group methods one could for instance investigate the effect of the band shape on the leading correlation-driven instabilities [12]. Moreover, the possibility that a longer hopping-range leads to better screening of the Coulomb repulsion, maybe even to overscreening, could be studied. Increased diagonal hopping, t', might lead to higher $T_{c\,\max}$ by suppression of static stripe order [13]. The Van Hove scenario [14] finds no support in Fig. 7 because it is the saddlepoint of the *anti*-bonding band which is at the LDA Fermi level in $YBa_2Cu_3O_7$; the bonding band is about half-filled and enhances spin-fluctuations with $\mathbf{q} \approx (\pi, \pi)$ [15]. The propensity to buckling is increased by pushing the conduction band towards the $O_{a/b}\, p_z$-level [5] by lowering of ε_s, but recent structural studies [9], as well as Fig. 7, disprove that static buckling enhances $T_{c\,\max}$, although dynamical buckling might. The inter-layer pair-tunnelling mechanism [16] is ruled out by the facts that $T_{c\max} \sim 90\,\mathrm{K}$ in both bct $Tl_2Ba_2CuO_6$ and simple tetragonal $HgBa_2CuO_4$ although the additional factor $\cos\frac{1}{2}k_x \cos\frac{1}{2}k_y$ attained by $t^{\perp}(\mathbf{k})$ in bct materials strongly suppresses the pair-tunnelling. That the axial orbital is *the* channel for coupling the layer to its surroundings is supported [17] by the observations that the **k**-dependence of the scattering in the normal state is v^2-like [6], and that c-axis transport is strongly suppressed by the opening of a pseudogap with similar **k**-dependence [18]. The axial orbital is also *the* non-correlated vehicle for coupling between oxygens in the layer. It therefore seems plausible that contraction of the axial orbital around the CuO_2-layer, away from the non-stoichiometric layers, will strengthen the phase coherence and thus increase $T_{c\max}$. Thermal excitation of nodal quasiparticles [19], on the other hand, seems not to be the mechanism by which HTSC is destroyed, because the axial orbital does not influence the band in the nodal direction. Finally, we mention that the correlation between r and $T_{c\,\max}$ does not extend to electron-doped cuprates, where the mechanism for superconductivity thus seems to be different.

References

[*] Present Addresses: $*$INFM-Dipartimento di Fisica, Via Bassi 6, I-27100, Italy. †IIT Bombay, Mumbai 400 076, India. ‡ S.N. Bose Centre, Kolkata 98, India.

[1] E. Pavarini *et al.*, Phys. Rev. Lett. **87**, 047003 (2001).

[2] For a recent review, see J. Orenstein and A.J. Millis, Science **288**, 468 (2000).

[3] V.J. Emery and S.A. Kivelson, Nature **374**, 434 (1995)

[4] J.-P. Locquet *et al.* Nature **394**, 453 (1998); H. Sato *et al.,* Phys. Rev. **61**, 12 447 (2000).

[5] O.K. Andersen *et al.*, J. Phys. Chem. Solids **56**, 1573 (1995).

[6] Z.X. Shen and D.S. Dessau, Phys. Rep **253**,1 (1995); H.H. Fretwell *et al.*, Phys. Rev. Lett. **84**, 4449 (2000); S.V. Borisenko *et al.*, Phys. Rev. Lett. **84**, 4453 (2000).

[7] O.K. Andersen *et al.*, Phys. Rev. B **62**, R16219 (2000); Psi-k Newsletter #45, 86 (June 2001); "Developing the MTO formalism" in *Electronic Structure and Physical Properties of Solids. The Uses of the LMTO Method,* ed. H. Dreyssé. Berlin/Heidelberg: Springer (2000). Lect. Notes Phys. 535 3-84, 2000.

[8] I. Dasgupta *et al.* (to be published).

[9] D. Godschmidt *et al.*, Phys. Rev. B **48**, 532 (1993); O. Chmaissem *et al.*, Nature **397,** 45 (1999).

[10] C.W. Chu *et al.,* Nature **365**, 323 (1993); M. Nunez-Regueiro *et al.,* Science **262**, 97 (1993).

[11] This is consistent with the observation of bilayer splitting: D.L. Feng *et al.*, Phys. Rev. Lett. **86**, 5550 (2001); Y.D. Chuang *et al.,* cond-mat/0102386.

[12] C.J. Halboth and W. Metzner, Phys. Rev. B **61**, 7364 (2000); C. Honerkamp *et al.,* cond-mat/9912358.

[13] M. Fleck *et al.,* cond-mat/0102041.

[14] D.M. Newns *et al.*, Com.Cond.Mat.Phys. **15,** 273 (1992)

[15] V.S. Oudovenko *et al.,* Physica C **336**, 157 (2000)

[16] S. Chakravarty *et al.,* Science **261**, 337 (1993).

[17] A.Z. Zheleznyak *et al.,* Phys.Rev. B **57**, 3089 (1998); L.B. Ioffe and A.J. Millis, Phys. Rev. B **58,** 11631 (1998).

[18] D. Basov *et al.*, Phys. Rev. B **50**, 3511 (1994); C.C. Holmes *et al.*, Physica C **254**, 265 (1995).

[19] P.A. Lee and X.G. Wen, Phys. Rev. Lett. **78**, 4111 (1997)